Contents lists available at ScienceDirect

# Physics Letters B

www.elsevier.com/locate/physletb

ELSEVIER

PHYSICS LETTERS B

# Mirror & hidden sector dark matter in the light of new CoGeNT data

R. Foot

*ARC Centre of Excellence for Particle Physics at the Terascale, School of Physics, University of Melbourne, Victoria 3010, Australia*

## A R T I C L E  I N F O

## A B S T R A C T

The CoGeNT Collaboration has recently made available new data collected over a period of 15 months. In addition to more accurately measuring the spectrum of nuclear recoil candidate events they have announced evidence for an annual modulation signal. We examine the implications of these new results within the context of mirror/hidden sector dark matter models. We find that the new CoGeNT data can be explained within this framework with parameter space consistent with the DAMA annual modulation signal, and the null results of the other experiments. We also point out that the CoGeNT spectrum at low energies is observed to obey $dR/dE_R \propto 1/E_R^2$ which suggests that dark matter interacts via Rutherford scattering rather than the more commonly assumed contact (four-fermion) interaction.

© 2011 Elsevier B.V. Open access under CC BY license.

The CoGeNT experiment operating in the Soudan Underground Laboratory has been searching for light dark matter interactions with a low energy threshold P-type Point Contact germanium detector [1,2]. They have obtained a low energy spectrum which is not readily explainable in terms of known background sources, and is consistent with elastic scattering of light dark matter particles [3–5]. Recently, 15 months of data has been analyzed [2] which greatly improves the measurement of the low energy spectrum and appears to be annually modulated with a phase consistent with dark matter expectations [6]. This further strengthens the dark matter interpretation of the CoGeNT low energy spectrum.

The recent CoGeNT results also reinforce the long standing observation of the DAMA Collaboration of an annual modulation signal in their *NaI* detector [7,8]. The DAMA signal is extremely impressive with statistical significance of 8.9 sigma with phase and period in agreement with the dark matter expectations to high accuracy. Attempts to interpret the DAMA signal in terms of a hypothetical background have become more and more implausible, and there is ample reason to be confident that DAMA and now CoGeNT have observed dark matter.

The positive results of DAMA and CoGeNT together with the null results of very sensitive, but higher threshold experiments such as CDMS [9] and XENON100 [10] suggest that dark matter is light ($\lesssim 30$ GeV). Having dark matter light, has long been known to alleviate the tension between DAMA and the higher threshold experiments [11] (see also Ref. [12]). However, the sensitivity of the higher threshold experiments has got to the point where there is now some tension between DAMA/CoGeNT and e.g. XENON10. XENON100, CDMS/Si, CDMS/Ge when interpreted in terms of standard WIMPs even if they are light [13]. Another issue is that the allowed parameter regions for the DAMA and CoGeNT signals, although close together do not significantly overlap in the standard WIMP framework [5]. It turns out that both of these difficulties can be resolved if dark matter is not only light, but assumed to be multi-component and self interacting.

A generic example of this [14] is dark matter from a hidden sector, which contains an unbroken $U(1)'$ gauge interaction which is mixed with the standard $U(1)_Y$ via renormalizable kinetic mixing interaction [15]:

$$\mathcal{L}_{mix} = \frac{\epsilon'}{2\cos\theta_w} F^{\mu\nu} F'_{\mu\nu} \tag{1}$$

where $F_{\mu\nu}$ is the standard $U(1)_Y$ gauge boson field strength tensor, and $F'_{\mu\nu}$ is the field strength tensor for the hidden sector $U(1)'$. This interaction enables hidden sector $U(1)'$ charged particles (of charge $Qe$) to couple to ordinary photons with electric charge $Q\epsilon'e \equiv \epsilon e$. We consider the case where the hidden sector contains two (or more) stable $U(1)'$ charged dark matter particles, $F_1$ and $F_2$ with masses $m_1$ and $m_2$ [$F_1$ and $F_2$ can be fermionic or bosonic]. Under the standard assumptions of a dark halo forming an isothermal sphere the condition of hydrostatic equilibrium relates the temperature of the particles to the galactic rotational velocity, $v_{rot}$:

$$T = \frac{1}{2}\bar{m} v_{rot}^2 \tag{2}$$

where $\bar{m} \equiv \frac{n_{F_1} m_1 + n_{F_2} m_2}{n_{F_1} + n_{F_2}}$ is the mean mass of the particles in the galactic halo. We have assumed that the self interactions mediated by the unbroken $U(1)'$ gauge interactions are sufficiently strong so that they thermalize the hidden sector particles, $F_1$ and $F_2$.

*E-mail address:* rfoot@unimelb.edu.au.

The interaction length is typically much less than a parsec [16] and the dark matter particles form a pressure-supported halo. The dark matter particles are then described by a Maxwellian distribution with $f_i(v) = \exp(-E/T) = \exp(-\frac{1}{2}m_i v^2/T) = \exp[-v^2/v_0^2(i)]$ where

$$v_0(i) = v_{rot}\sqrt{\frac{\bar{m}}{m_i}}. \tag{3}$$

With the assumptions that $m_2 \gg m_1$ and that the abundance of $F_2$ is much less than $F_1$, we have that $v_0^2(F_2) \ll v_{rot}^2$. The narrow velocity dispersion (recall $\sigma_v^2 = 3v_0^2/2$) can greatly reduce the rate of dark matter interactions in higher threshold experiments such as XENON100 whilst still explaining the signals in the lower threshold DAMA and CoGeNT experiments.

While generic hidden sector models are interesting in their own right and have been studied in some detail (see e.g. Ref. [17]), I consider mirror dark matter as the best motivated example of such a multi-component self-interacting theory. Recall, mirror dark matter posits that the inferred dark matter in the Universe arises from a hidden sector which is an exact copy of the standard model sector [18] (for a review and more complete list of references see Ref. [19]).[1] That is, a spectrum of dark matter particles of known masses are predicted: $e'$, $H'$, $He'$, $O'$, $Fe'$, ... (with $m_{e'} = m_e$, $m_{H'} = m_H$, etc.). The galactic halo is then presumed to be composed predominantly of a spherically distributed self interacting mirror particle plasma comprising these particles [21]. Kinetic mixing of the $U(1)_Y$ and its mirror counterpart allows ordinary and mirror particles to interact with each other and can thereby explain the direct detection experiments [3,4,11]. The simplest scenario involves kinetic mixing induced elastic (Rutherford) scattering of the dominant mirror metal component, $A'$, off target nuclei. [The $He'$ and $H'$ components are too light to give a signal above the DAMA/CoGeNT energy threshold.] Previous work [3,4] (see also Refs. [11,14]) has shown that such elastic scattering can explain the normalization and energy dependence of the DAMA annual modulation amplitude and also the initial (56 days) CoGeNT spectrum consistently with the null results of the other experiments, and yields a measurement of $\epsilon\sqrt{\xi_{A'}}$ and $m_{A'}$:

$$\epsilon\sqrt{\xi_{A'}} \approx (7 \pm 3) \times 10^{-10},$$
$$\frac{m_{A'}}{m_p} \approx 22 \pm 8 \tag{4}$$

where $\xi_{A'} \equiv n_{A'}m_{A'}/(0.3~\text{GeV/cm}^3)$ is the halo mass fraction of the species $A'$ and $m_p$ is the proton mass. The measured value of $m_{A'}/m_p$ is consistent with $A' \sim O'$, which by analogy with the ordinary matter sector would be the naive expectation. Taking a range for $\xi_{A'}$, $1 \gtrsim \xi_{A'} \gtrsim 10^{-2}$, suggests that $\epsilon$ could realistically range from $10^{-10}$ to $10^{-8}$. Kinetic mixing in this range is consistent with laboratory and astrophysical constraints [22] and has a number of fascinating applications [22,19,23]. Early Universe cosmology, though, prefers [24] $\epsilon \lesssim 10^{-9}$.

The interaction rate in experiments depends on the halo distribution function and the interaction cross-section. The former is expected to be a Maxwellian distribution, $f_i(v) = \exp[-v^2/v_0^2(i)]$, with $v_0(i)$ depending on $\bar{m}$, as discussed above. In the mirror dark matter case, $\bar{m}$ is expected to be around 1 GeV, but with significant uncertainties [3,4]. Generally it has been found [3] that the dark matter detection experiments are relatively insensitive to the precise value of $v_0(A')$ (and hence $\bar{m}$) so long as $v_0^2(A') \ll v_{rot}^2$. Kinetic

mixing induced elastic Rutherford scattering is particularly natural in mirror/hidden sector models as it arises from the renormalizable interaction, Eq. (1). In the present study we again assume that it is the dominant interaction mechanism coupling ordinary and dark matter. The cross-section for a dark matter particle of charge $\epsilon e$ to elastically scatter off an ordinary nucleus (presumed at rest with mass and atomic numbers $A$, $Z$) is given by [11][2]:

$$\frac{d\sigma}{dE_R} = \frac{\lambda}{E_R^2 v^2} \tag{5}$$

where

$$\lambda \equiv \frac{2\pi\epsilon^2 Z^2\alpha^2}{m_A}F_A^2(qr_A) \tag{6}$$

and $F_A(qr_A)$ is the form factor which takes into account the finite size of the nuclei. In the case where dark matter particles also have finite size, as in the mirror dark matter case, a form factor for those particles also needs to be included. [For elastic scattering of mirror nuclei, $A'$, of atomic number $Z'$ we must replace $\epsilon \to Z'\epsilon$ in the above cross-section formula]. A simple analytic expression for the form factor, which we adopt in our numerical work, is the one proposed by Helm [25,26].

The event rate is given by:

$$\frac{dR}{dE_R} = N_T n_{A'} \int_{|\mathbf{v}|>v_{min}}^{\infty} \frac{d\sigma}{dE_R}\frac{f_{A'}(\mathbf{v},\mathbf{v}_E)}{k}|\mathbf{v}|\,d^3v \tag{7}$$

where $N_T$ is the number of target nuclei per kg of detector and $n_{A'} = \rho_{dm}\xi_{A'}/m_{A'}$ is the number density of halo dark matter particles $A'$ at the Earth's location (we take $\rho_{dm} = 0.3~\text{GeV/cm}^3$). Here $\mathbf{v}$ is the velocity of the halo particles relative to the Earth and $\mathbf{v}_E$ is the velocity of the Earth relative to the galactic halo. The integration limit, $v_{min}$, is given by the kinematic relation:

$$v_{min} = \sqrt{\frac{(m_A + m_{A'})^2 E_R}{2m_A m_{A'}^2}}. \tag{8}$$

The halo distribution function in the reference frame of the Earth is given by, $f_{A'}(\mathbf{v},\mathbf{v}_E)/k = (\pi v_0^2[A'])^{-3/2}\exp(-(\mathbf{v}+\mathbf{v}_E)^2/v_0^2[A'])$. The integral, Eq. (7), can easily be evaluated in terms of error functions [14,26] and numerically solved.

To compare with the measured event rate, we must include detector resolution effects and overall detection efficiency (when the latter is not already included in the experimental results):

$$\frac{dR}{dE_R^m} = \epsilon_f(E_R^m)\frac{1}{\sqrt{2\pi}\sigma_{res}}\int\frac{dR}{dE_R}e^{-(E_R-E_R^m)^2/2\sigma_{res}^2}dE_R \tag{9}$$

where $E_R^m$ is the measured energy and $\sigma_{res}$ describes the resolution. The measured energy is typically in keVee units (ionization/scintillation energy). For nuclear recoils in the absence of any channeling, keVee $=$ keV/$q$, where $q < 1$ is the relevant quenching factor. Channeled events, where target atoms travel down crystal axis and planes, have $q \simeq 1$. In light of recent theoretical studies [27], we assume that the channeling fraction is negligible. It is of course still possible that channeling could play some role, which could modify the favoured regions of parameter space somewhat.

For this study we consider two of the simplest examples of multi-component dark matter models. Following our earlier works [3,4,14,11] we consider mirror dark matter with a dominant mirror

---

[1] Note that successful big bang nucleosynthesis and successful large scale structure requires effectively asymmetric initial conditions in the early Universe, $T' \ll T$ and $n_{b'}/n_b \approx 5$. See Ref. [20] for further discussions.

[2] We employ natural units where $\hbar = c = 1$.
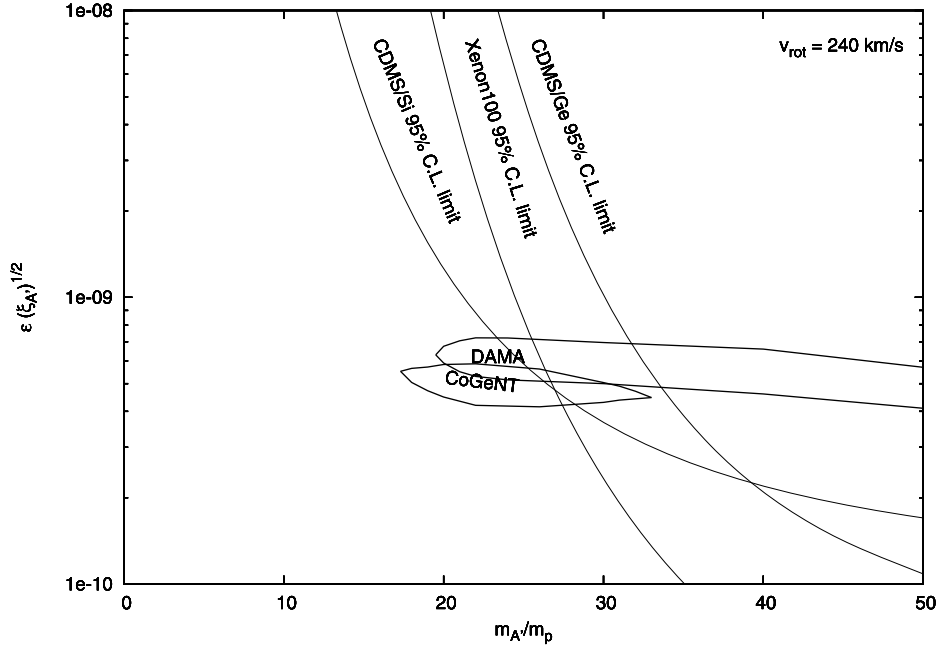
**Fig. 1.** CoGeNT and DAMA 99% C.L. favoured parameter $(m_{A'}, \epsilon\sqrt{\xi_{A'}})$ regions for the mirror dark matter model. The reference point $v_{rot} = 240$ km/s is assumed. Also shown are the 95% exclusion curves evaluated from the null results of XENON100, CDMS/Si and CDMS/Ge.

metal component, $A'$, of atomic number $Z'$. In this case the electric charge of the dark matter particle is $\epsilon Z'e$.[3] The quantity $v_0(A')$ is obtained from Eq. (3) with $\bar{m} \simeq 1.1$ GeV, which corresponds to a He$'$ dominated halo, $Y_{He'} \simeq 0.9$, expected [28] for $\epsilon \sim 10^{-9}$. We also consider the more generic two component $F_1$, $F_2$ hidden sector dark matter model discussed above, in which case $v_0$ is less constrained.

One can define a $\chi^2$ quantity and compare these theories with experiment. We consider the reference point $v_{rot} = 240$ km/s which is representative of recent measurements for the local rotational velocity [29]. The data we consider consists of (a) the CoGeNT energy spectrum: 31 bins of width $\Delta E \simeq 0.05$ keVee given in the inset of Fig. 1 of Ref. [2]. This spectrum has already been corrected for efficiency and stripped of background components. (b) The DAMA annual modulation energy spectrum in the energy range $2 < E(\text{keVee}) < 8$. We have taken into account systematic uncertainties in energy scale by minimizing $\chi^2$ over a 20% variation in quenching factors, i.e. $q_{Na} = 0.30 \pm 0.06$, $q_I = 0.09 \pm 0.02$ for DAMA and $q_{Ge} = 0.21 \pm 0.04$ for CoGeNT. The mirror dark matter candidate provides an excellent fit to the data, with $\chi^2_{min}/\text{d.o.f.}$ values of 23.1/29 for data set (a), and 8.9/10 for data set (b).[4] Favoured regions in the $\epsilon\sqrt{\xi_{A'}}$, $m_{A'}$ plane can be obtained by evaluating contours corresponding to $\chi^2(\epsilon\sqrt{\xi_{A'}}, m_{A'}) = \chi^2_{min} + 9$ (roughly 99% C.L. allowed region). In Fig. 1 we show the parameter regions favoured by the data for the $v_{rot} = 240$ km/s reference point. The favoured regions for the DAMA and CoGeNT signals are in as good an agreement as one might expect given the systematic

uncertainties which we have not considered including the fiducial bulk volume uncertainty in CoGeNT of $\sim 10\%$ and variation of $v_{rot}$ within its estimated $\sim 10\%$ uncertainty.

Also displayed in Fig. 1 is the 95% exclusion limits evaluated for the CDMS/Si [31], CDMS/Ge [9] and XENON100 [10] experiments.[5] In computing these limits, we have conservatively taken the energy thresholds of these experiments to be 20% higher than the advertised values, to allow for systematic uncertainties in energy calibration and quenching factor.[6] We also show in Fig. 2(a), (b), the predicted results for each data set for a particular parameter point near the global best fit, as well as a point near the best fit for each data set considered separately.

It is interesting to compare the 15 month CoGeNT favoured region, as shown in Fig. 1, with results for the same model obtained with the initial 56 days of data [3,4]. The current favoured region is significantly reduced in size. CoGeNT data now feature an upper limit on $m_{A'} \lesssim 30$ GeV, which is also supported by the null results of XENON100 and CDMS/Si.

The CoGeNT Collaboration report [2] evidence for an annual modulation signal in their data at about $2.8\sigma$ C.L. The amplitude of the modulation, averaged over $0.5 < E(\text{keVee}) < 3.0$, is measured to be roughly $A \approx 0.46 \pm 0.17$ cpd/kg/keVee. This assumes the amplitude and phase are set to theoretical expectations, while a larger amplitude is preferred if the phase is left free. For the theories offered here, we find that the CoGeNT annual modulation amplitude (averaged over $0.5 < E(\text{keVee}) < 3.0$) is typically around $\sim 0.12$ cpd/kg/keVee for the parameter region near the global best fit, and does not get above 0.20 for any parameter point in the global 99% C.L. favoured parameter region (for the reference point $v_{rot} = 240$ km/s). Thus we find an annual modulation somewhat

---

[3] In our numerical work we allow $A'$, $Z'$, to have non-integer values, with $Z' = A'/2$. Since the realistic case will involve a spectrum of elements, the effective mass can be non-integer.

[4] The low CoGeNT threshold of 0.45 keVee potentially makes the experiment sensitive to the $e'$ component via $e'$-electron scattering, which would be expected to lead to a large rise in event rate at low energies [30]. The data is adequately fit by $A' - Ge$ elastic scattering, with no evidence for an extra $e' - e$ scattering contribution. This suggests that the $e'$ halo component has a lower temperature than the mirror nuclei component. Such a scenario is possible due to the inefficient energy transfer between the light $e'$ and much heavier mirror nuclei.

[5] There are also lower threshold analysis by XENON10 [32] and CDMS [33] collaborations. However when systematic uncertainties are properly incorporated, neither analysis is capable of excluding light dark matter explanations of the DAMA/CoGeNT signal [34].

[6] Within the mirror dark matter framework the higher threshold experiments such as CDMS/Ge and XENON100 have an important role in probing the heavier $\sim$ Fe$'$ component [35].
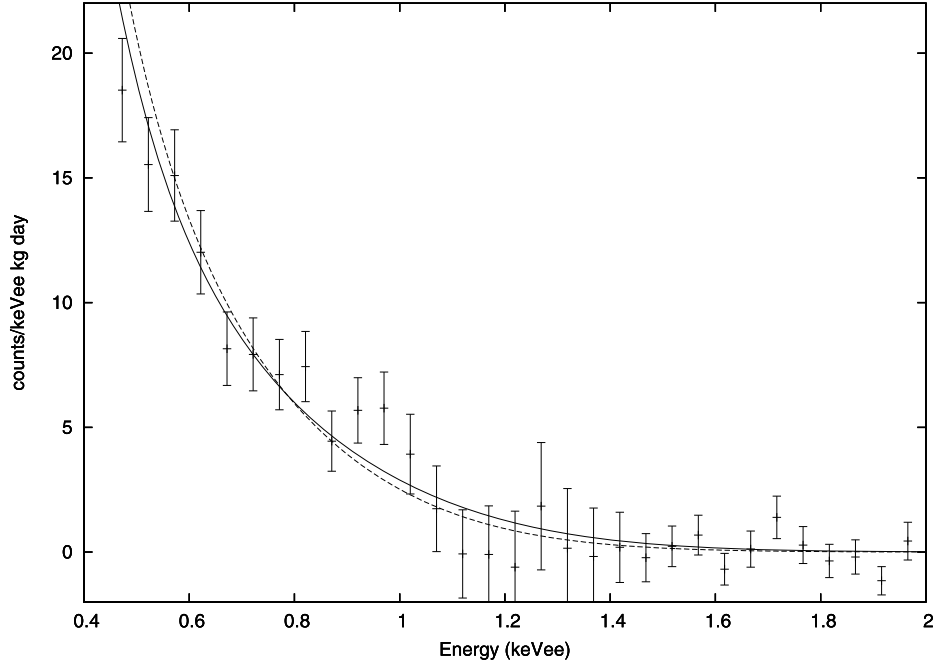
(a) Mirror dark matter versus the CoGeNT spectrum. The solid line is for a point near the CoGeNT best fit $[m_{A'}/m_p = 26, \epsilon\sqrt{\xi_{A'}} = 5.2 \times 10^{-10}]$ while the dashed line is for a point near the global best fit $[m_{A'}/m_p = 24, \epsilon\sqrt{\xi_{A'}} = 5.7 \times 10^{-10}]$.
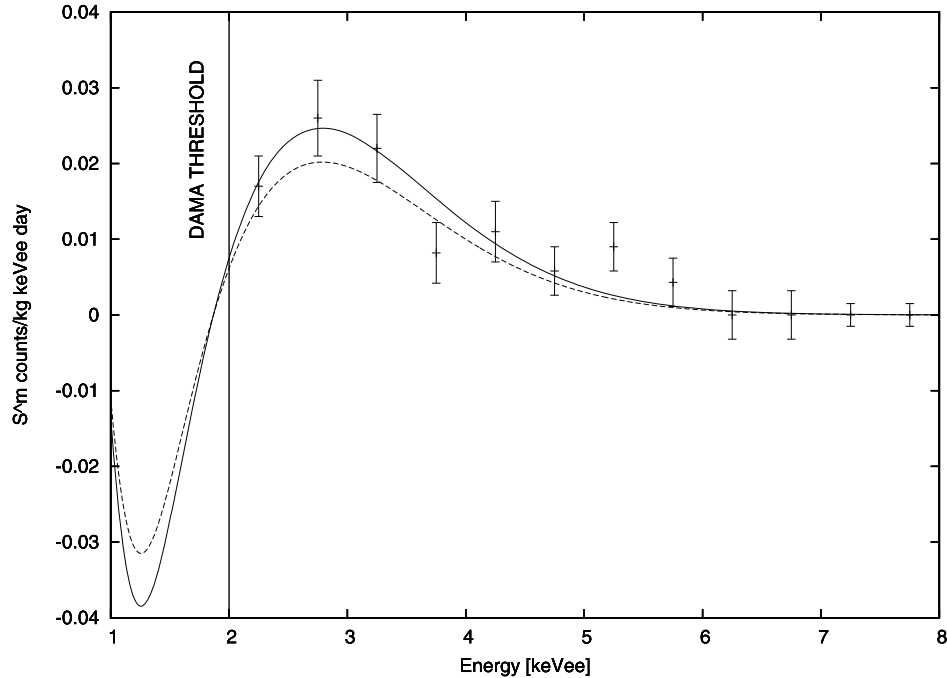


(b) Mirror dark matter versus the DAMA annual modulation spectrum. The solid line is for a point near the DAMA best fit $[m_{A'}/m_p = 24, \epsilon\sqrt{\xi_{A'}} = 6.3 \times 10^{-10}]$ while the dashed line is for the point near the global best fit considered in (a) $[m_{A'}/m_p = 24, \epsilon\sqrt{\xi_{A'}} = 5.7 \times 10^{-10}]$.

**Fig. 2.**

below the CoGeNT central value. This difference, though, is not currently, statistically significant, representing only a 1.5–2 sigma downward fluctuation from the central value measured in the 15 × 0.33 month-kg data sample. Obviously future data, especially the measurement of the energy spectrum of the annual modulation amplitude, will be important tests of the theories considered here.

Similar results hold for the more generic two component $F_1$, $F_2$ hidden sector dark matter model discussed earlier. For definiteness we have assumed the same $v_0$ value for $F_2$ (i.e. same $\bar{m}$ value) as for $A'$ in mirror dark matter. We have computed the $\chi^2$ as before, minimizing over systematic uncertainties in quenching factor. The best fit features $\chi^2_{min}$/d.o.f. values of 23.0/29 for the CoGeNT data set (a), and 9.2/10 for the DAMA data set (b). The parameter range
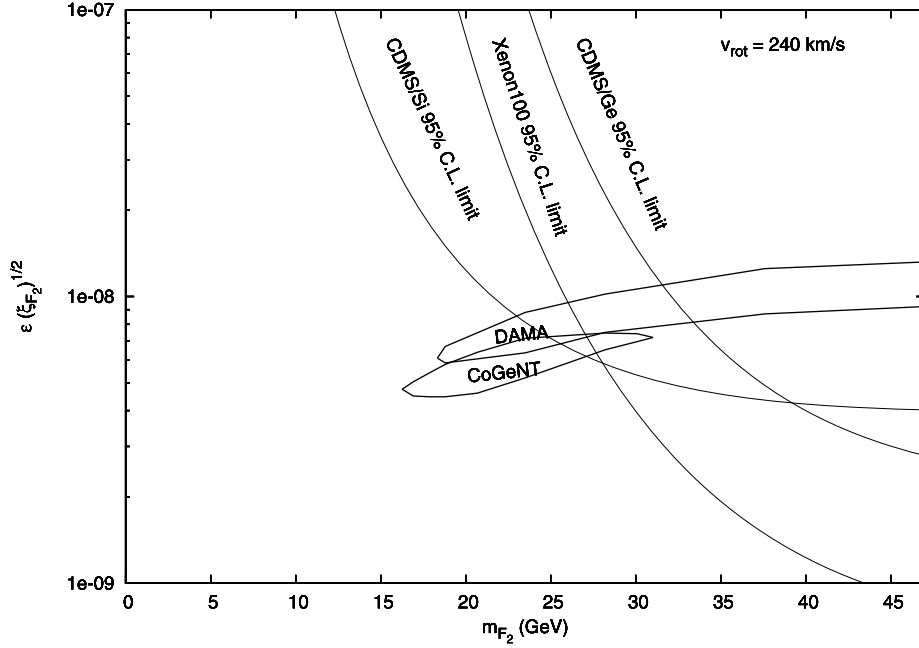
**Fig. 3.** CoGeNT and DAMA 99% C.L. favoured parameter ($m_{F_2}$, $\epsilon\sqrt{\xi_{F_2}}$) regions for the generic hidden sector dark matter model discussed in the text. The reference point $v_{rot} = 240$ km/s is assumed. Also shown are the 95% exclusion curves evaluated from the null results of the XENON100, CDMS/Si and CDMS/Ge experiments.

favoured by the CoGeNT and DAMA data sets (a) and (b) discussed above is given in Fig. 3 for this case. Note that since the electric charge of $F_2$ is $\epsilon e$ rather than $Z'\epsilon e$ the allowed region is shifted c.f. the mirror matter case: $\epsilon \leftrightarrow \epsilon/Z'$. We have also found that the model can fit the data for a wide range of $v_0(i)$ values: $v_0(i) \lesssim 140$ km/s.

The explanation of the DAMA/LIBRA and CoGeNT experiments considered here has a number of interesting features. As noted previously [4] the signals seen in these experiments arise predominately from dark matter particle interactions in the body of their Maxwellian velocity distribution rather than the tail (as in the model of Refs. [12,5]). Because of this, we do not have a great deal of freedom in modifying the predicted shape of the spectrum, and thus the agreement of the model with the spectrum observed by CoGeNT is a non-trivial test of the theory. In fact in the $v_0^2(A')/v_{rot}^2 \to 0$ limit, the energy dependence of $dR/dE_R$ [Eq. (7)] follows exactly that of $d\sigma/dE_R$ and is proportional to $1/E_R^2$ for $v_{min} < v_{rot}$ and $d\sigma/dE_R = 0$ for $v_{min} > v_{rot}$. [Excepting here the energy dependence of the form factor which is relatively minor for $E_R \lesssim 1$ keVee in germanium.] The $1/E_R^2$ dependence of $d\sigma/dE_R$ follows directly from the masslessness of the exchanged photon in the Feynman diagram describing the interaction and is thus a distinctive feature of dark matter interacting via Rutherford scattering. For finite $v_0(A')/v_{rot}$ the $1/E_R^2$ behaviour is expected provided that $E_R$ is sufficiently small that $v_{min} \lesssim v_{rot}$, i.e. for

$$E_R \lesssim \frac{2m_A m_{A'}^2}{(m_A + m_{A'})^2} v_{rot}^2. \tag{10}$$

For $A = Ge$, $v_{rot} = 240$ km/s and $m_{A'} \gtrsim 18$ GeV (the latter suggested by the fit to the DAMA annual modulation signal), we have

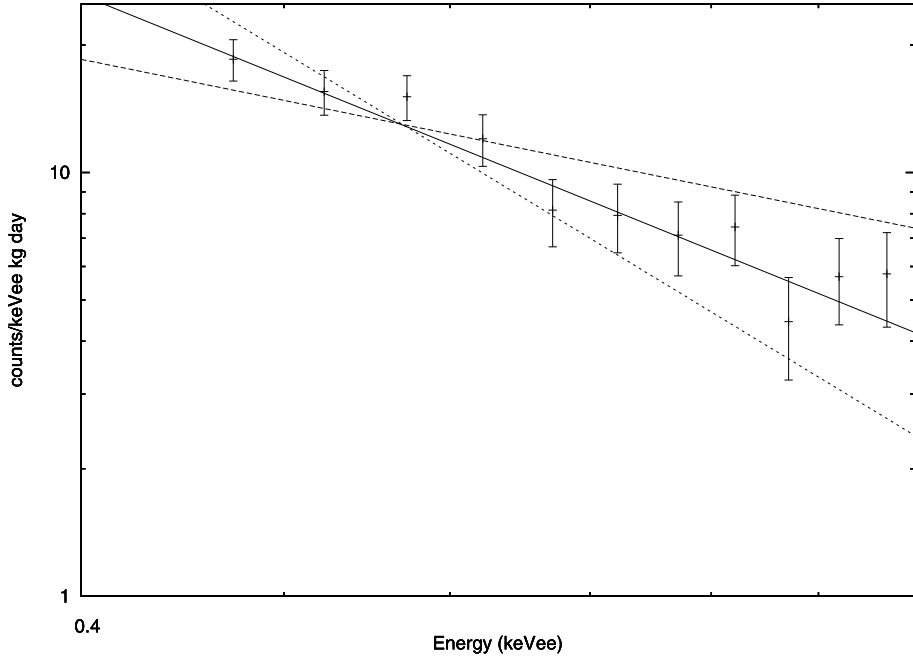$$\frac{dR}{dE_R} \propto \frac{1}{E_R^2} \tag{11}$$

for $E_R \lesssim 1$ keVee. This prediction is impressively consistent with the observations as indicated in Fig. 4. CoGeNT's spectrum falls off more rapidly than $1/E_R^2$ at $E_R \gtrsim 1$ keVee. This suggests the onset

of the kinematic threshold $v_{min} \gtrsim v_{rot}$ at these energies and is the origin of the $m \lesssim 30$ GeV upper limit indicated in Figs. 1, 3.

The dark matter explanation of CoGeNT's spectrum offered here can be compared with the model of Refs. [12,5] which features WIMPS elastically scattering via a contact (four fermion) interaction rather than via Rutherford scattering. The contact interaction produces a flat (in $E_R$) cross-section, excepting the mild (at these energies) recoil energy dependence of the form factor. A rapidly falling spectrum would then only be expected if dark matter particles are so light that only particles in the tail of the halo velocity distribution can lead to recoils with enough energy to be observed. In such a scenario the shape of the $dR/dE_R$ spectrum necessarily depends very sensitively on $m_{wimp}$. Only for $m_{wimp} \simeq 7.0$ GeV (and with standard assumptions) [2] can that model account for the observed spectrum energy dependence $dR/dE_R \sim 1/E_R^2$ at low $E_R$. However the energy dependence is accommodated, rather than explained, which is in contrast to the Rutherford scattering scenarios considered here.

Future experiments should be able to more clearly distinguish mirror/hidden sector models from other theoretical explanations — such as the one discussed in Refs. [12,5] and many others considered in recent literature — by e.g. precise measurements of the annual modulation energy spectrum. The mirror/hidden sector models predict a characteristic change in sign of the annual modulation amplitude at low energies (see Fig. 6 of Ref. [4]). Distinguishing the mirror dark matter case from the more generic hidden sector model might prove more challenging. Whilst the two theories give essentially identical results for the DAMA/CoGeNT experiments mirror dark matter predicts a spectrum of particles of known masses. In particular the scattering of low mass components, $e'$ on electrons and He'/H' on target nuclei can ultimately be seen in very low threshold experiments. Higher mass subcomponents, such as a $\sim$ Fe' or $\sim$ Ca' component would also be expected and should ultimately be observed if dark matter is of the mirror type.

In conclusion, we have examined mirror/hidden sector dark matter in the light of CoGeNT's more precisely measured spectrum

**Fig. 4.** Low energy CoGeNT spectrum compared with $dR/dE_R \propto 1/E_R^n$ where $n=1$ (dashed line), $n=2$ (solid line) and $n=3$ (dotted line). The data clearly favour the $n=2$ case, which is expected in the mirror dark matter/hidden sector models considered here, and is characteristic of dark matter interacting via elastic Rutherford scattering.

and annual modulation signal [2]. The CoGeNT spectrum is observed to obey $dR/dE_R \propto 1/E_R^2$ at low energies which suggests that dark matter interacts via a massless or light mediator (Rutherford scattering) rather than the more commonly assumed contact (four-fermion) interaction. Such Rutherford scattering is a feature of mirror and more generic hidden sector dark matter models considered here and in previous works [3,4,14,11]. We have found that such models provide an excellent fit to the data which is easily consistent with the null results of the sensitive but higher threshold experiments, such as CDMS and XENON100. The next generation P-type Point Contact detectors, including CoGeNT(C-4), MAJORANA, GERDA and CDEX should be able to provide a decisive test of these models by e.g. a precise measurement of the annual modulation energy spectrum. These and other experiments are awaited with interest.

### Acknowledgement

### References

[1] C.E. Aalseth, et al., CoGeNT Collaboration, Phys. Rev. Lett. 106 (2011) 131301, arXiv:1002.4703.
[2] C.E. Aalseth, et al., CoGeNT Collaboration, arXiv:1106.0650.
[3] R. Foot, Phys. Lett. B 692 (2010) 65, arXiv:1004.1424.
[4] R. Foot, Phys. Rev. D 82 (2010) 095001, arXiv:1008.0685.
[5] D. Hooper, J.I. Collar, J. Hall, D. McKinsey, Phys. Rev. D 82 (2010) 123509, arXiv:1007.1005.
[6] A.K. Drukier, K. Freese, D.N. Spergel, Phys. Rev. D 33 (1986) 3495;
    K. Freese, J.A. Frieman, A. Gould, Phys. Rev. D 37 (1988) 3388.
[7] R. Bernabei, et al., DAMA Collaboration, Riv. Nuovo Cimento. 26 (2003) 1, astro-ph/0307403;
    R. Bernabei, et al., DAMA Collaboration, Int. J. Mod. Phys. D 13 (2004) 2127;
    R. Bernabei, et al., DAMA Collaboration, Phys. Lett. B 480 (2000) 23.
[8] R. Bernabei, et al., DAMA Collaboration, Eur. Phys. J. C 56 (2008) 333, arXiv:0804.2741;
    R. Bernabei, et al., DAMA Collaboration, Eur. Phys. J. C 67 (2010) 39, arXiv:1002.1028.

[9] Z. Ahmed, et al., CDMS Collaboration, Science 327 (2010) 1619, arXiv:0912.3592.
[10] E. Aprile, et al., XENON100 Collaboration, arXiv:1104.3121.
[11] R. Foot, Phys. Rev. D 69 (2004) 036001, hep-ph/0308254;
     R. Foot, astro-ph/0403043;
     R. Foot, Mod. Phys. Lett. A 19 (2004) 1841, astro-ph/0405362;
     R. Foot, Phys. Rev. D 74 (2006) 023514, astro-ph/0510705.
[12] P. Gondolo, G. Gelmini, Phys. Rev. D 71 (2005) 123520, hep-ph/0504010.
[13] C. Savage, G. Gelmini, P. Gondolo, K. Freese, Phys. Rev. D 83 (2011) 055002, arXiv:1006.0972.
[14] R. Foot, Phys. Rev. D 78 (2008) 043529, arXiv:0804.4518.
[15] R. Foot, X.-G. He, Phys. Lett. B 267 (1991) 509.
[16] R. Foot, Phys. Lett. B 699 (2011) 230, arXiv:1011.5078.
[17] J.L. Feng, M. Kaplinghat, H. Tu, H.-B. Yu, JCAP 0907 (2009) 004, arXiv:0905.3039.
[18] R. Foot, H. Lew, R.R. Volkas, Phys. Lett. B 272 (1991) 67;
     R. Foot, H. Lew, R.R. Volkas, Mod. Phys. Lett. A 7 (1992) 2567.
[19] R. Foot, Int. J. Mod. Phys. D 13 (2004) 2161, astro-ph/0407623;
     P. Ciarcelluti, Int. J. Mod. Phys. D 19 (2010) 2151, arXiv:1102.5530.
[20] H.M. Hodges, Phys. Rev. D 47 (1993) 456;
     Z. Berezhiani, D. Comelli, F.L. Villante, Phys. Lett. B 503 (2001) 362, hep-ph/0008105;
     L. Bento, Z. Berezhiani, Phys. Rev. Lett. 87 (2001) 231304, hep-ph/0107281;
     A.Yu. Ignatiev, R.R. Volkas, Phys. Rev. D 68 (2003) 023518, hep-ph/0304260;
     R. Foot, R.R. Volkas, Phys. Rev. D 68 (2003) 021304, hep-ph/0304261;
     R. Foot, R.R. Volkas, Phys. Rev. D 69 (2004) 123510, hep-ph/0402267;
     Z. Berezhiani, P. Ciarcelluti, D. Comelli, F.L. Villante, Int. J. Mod. Phys. D 14 (2005) 107, astro-ph/0312605;
     P. Ciarcelluti, Int. J. Mod. Phys. D 14 (2005) 187, astro-ph/0409630;
     P. Ciarcelluti, Int. J. Mod. Phys. D 14 (2005) 223, astro-ph/0409633;
     For pioneering work, see: S.I. Blinnikov, M.Yu. Khlopov, Sov. J. Nucl. Phys. 36 (1981) 472;
     S.I. Blinnikov, M.Yu. Khlopov, Sov. Astron. 27 (1983) 371.
[21] R. Foot, R.R. Volkas, Phys. Rev. D 70 (2004) 123508, astro-ph/0407522.
[22] R. Foot, A.Yu. Ignatiev, R.R. Volkas, Phys. Lett. B 503 (2001) 355, astro-ph/0011156;
     R. Foot, Int. J. Mod. Phys. A 19 (2004) 3807, astro-ph/0309330;
     R. Foot, Z.K. Silagadze, Int. J. Mod. Phys. D 14 (2005) 143, astro-ph/0404515;
     R. Foot, Phys. Lett. B 699 (2011) 230, arXiv:1011.5078;
     See also, S. Davidson, S. Hannestad, G. Raffelt, JHEP 0005 (2000) 3, hep-ph/0001179.
[23] R. Foot, S. Mitra, Astropart. Phys. 19 (2003) 739, astro-ph/0211067;
     R. Foot, S. Mitra, Phys. Lett. A 315 (2003) 178, cond-mat/0306561;
     R. Foot, S. Mitra, Phys. Lett. B 558 (2003) 9, astro-ph/0301229.
[24] P. Ciarcelluti, R. Foot, Phys. Lett. B 679 (2009) 278, arXiv:0809.4438.

[25] R.H. Helm, Phys. Rev. 104 (1956) 1466.
[26] J.D. Lewin, P.F. Smith, Astropart. Phys. 6 (1996) 87.
[27] N. Bozorgnia, G.B. Gelmini, P. Gondolo, JCAP 1011 (2010) 019, arXiv:1006.3110;
     N. Bozorgnia, G.B. Gelmini, P. Gondolo, JCAP 1011 (2010) 028, arXiv:1008.3676.
[28] P. Ciarcelluti, R. Foot, Phys. Lett. B 690 (2010) 462, arXiv:1003.0880.
[29] A. Brunthaler, et al., arXiv:1102.5350.
[30] R. Foot, Phys. Rev. D 80 (2009) 091701, arXiv:0909.3126.

[31] J.P. Filippini, Ph.D. thesis, 2008.
[32] J. Angle, et al., XENON10 Collaboration, arXiv:1104.3088.
[33] Z. Ahmed, et al., CDMS Collaboration, Phys. Rev. Lett. 106 (2011) 131302,
     arXiv:1011.2482.
[34] J.I. Collar, arXiv:1010.5187;
     J.I. Collar, arXiv:1103.3481.
[35] R. Foot, Phys. Rev. D 81 (2010) 087302, arXiv:1001.0096.